SMC-TR-05-03

AEROSPACE REPORT NO.
TR-2004(8570)-8

Focus and Tip-Tilt Alignment Procedure for the Enhanced Aerospace Near-Infrared Imaging Spectrograph

30 August 2004

Prepared by

R. J. RUDY and D. J. GUTIERREZ
Space Science Applications Laboratory
Laboratory Operations

Prepared for

SPACE AND MISSILE SYSTEMS CENTER
AIR FORCE SPACE COMMAND
2430 E. El Segundo Boulevard
Los Angeles Air Force Base, CA 90245

Engineering and Technology Group

THE AEROSPACE CORPORATION
El Segundo, California

This report was submitted by The Aerospace Corporation, El Segundo, CA 90245-4691, under Contract No. FA8802-04-C-0001 with the Space and Missile Systems Center, 2430 E. El Segundo Blvd., Los Angeles Air Force Base, CA 90245. It was reviewed and approved for The Aerospace Corporation by J. A. Hackwell, Principal Director, Space Science Applications Laboratory. Michael Zambrana was the project officer for the Mission-Oriented Investigation and Experimentation (MOIE) program.

This report has been reviewed by the Public Affairs Office (PAS) and is releasable to the National Technical Information Service (NTIS). At NTIS, it will be available to the general public, including foreign nationals.

This technical report has been reviewed and is approved for publication. Publication of this report does not constitute Air Force approval of the report's findings or conclusions. It is published only for the exchange and stimulation of ideas.

Michael Zambrana
SMC/AXE

REPORT DOCUMENTATION PAGE

Form Approved
OMB No. 0704-0188

1. REPORT DATE (*DD-MM-YYYY*)	2. REPORT TYPE	3. DATES COVERED *(From - To)*
08-30-2004		

4. TITLE AND SUBTITLE

Focus and Tip-Tilt Alignment Procedure for the Enhanced Aerospace Near-Infrared Imaging Spectrograph

5a. CONTRACT NUMBER
FA8802-04-C-0001

5b. GRANT NUMBER

5c. PROGRAM ELEMENT NUMBER

6. AUTHOR(S)

R. J. Rudy, D. J. Gutierrez

5d. PROJECT NUMBER

5e. TASK NUMBER

5f. WORK UNIT NUMBER

7. PERFORMING ORGANIZATION NAME(S) AND ADDRESS(ES)

The Aerospace Corporation
Laboratory Operations
El Segundo, CA 90245-4691

8. PERFORMING ORGANIZATION REPORT NUMBER

TR-2004(8570)-8

9. SPONSORING / MONITORING AGENCY NAME(S) AND ADDRESS(ES)

Space and Missile Systems Center
Air Force Space Command
2450 E. El Segundo Blvd.
Los Angeles Air Force Base, CA 90245

10. SPONSOR/MONITOR'S ACRONYM(S)
SMC

11. SPONSOR/MONITOR'S REPORT NUMBER(S)
SMC-TR-05-03

12. DISTRIBUTION/AVAILABILITY STATEMENT

Approved for public release; distribution unlimited.

13. SUPPLEMENTARY NOTES

14. ABSTRACT

This document describes the procedure used to assess focus of the enhanced Aerospace Near-Infrared Imaging Spectrograph (NIRIS). NIRIS is a long-slit spectrograph operating from 0.38 μm to 2.5 μm, but the procedure is applicable to almost all hyperspectral imagers. The procedure also assesses the orthogonality of the focal-plane arrays relative to the optical axis (i.e, tip-tilt = pitch and yaw) and provides information about the rotation of the array about the optical axis (i.e., roll) as well. These tasks are accomplished by observing an emission line lamp (or any other suitable wavelength calibration source) at opposite edges of the spectrograph's F-beam. This procedure requires only the emission lamp and the hyperspectral imager under test and provides quantitative measurements of the magnitude and direction of focus error as well as FPA non-orthogonality. Procedures for reducing and analyzing the data are included as well.

15. SUBJECT TERMS

Hyperspectral Imaging, Infrared Instrumentation

16. SECURITY CLASSIFICATION OF:			17. LIMITATION OF ABSTRACT	18. NUMBER OF PAGES	19a. NAME OF RESPONSIBLE PERSON
					Richard Rudy
a. REPORT	b. ABSTRACT	c. THIS PAGE			19b. TELEPHONE NUMBER *(include area code)*
UNCLASSIFIED	UNCLASSIFIED	UNCLASSIFIED		13	(310)336-5799

Acknowledgments

We wish to thank J. A. Hackwell and D. W. Warren for several helpful discussions and acknowledge D. W. Warren for the optical design for the NIRIS instrument. C. Venturini is thanked for her aid in preparing this document. This work was supported by the US Air Force Space and Missile Systems Center through the Mission Oriented Investigation and Experimentation program, under contract FA8802-04-C-0001.

Contents

1. Background and Theory 1
2. Measurement Procedure 5
3. Data Reduction Procedure 7
4. Data Analysis Procedure 9
5. Summary 13

Figures

1. Simplified schematic illustrating the concept for testing focus 2
2. Emission lamp power supply, bulb, and cover 2
3. Discharge lamp operating with He bulb 3
4. Right and left lamp positions for focus and orientation 5
5. Argon spectrum in the 0.9–1.3 μm range 7
6. Results from a focus measurement for the two infrared channels of NIRIS 9
7. Same as Figure 4 but with an optical bench temperature (160.5K) much closer to nominal .. 10

1. Background and Theory

The correct focus and proper alignment of the focal-plane array (FPA) is essential to the performance of hyperspectral imagers but can be difficult to achieve. Fast camera optics, small pixels, and physically large arrays all contribute to the need for precise FPA positioning with respect to the optics. We describe here a measurement conceived by one of us (DJG) for assessment of an LWIR sensor but applied here to The Aerospace Corporation's enhanced Near-Infrared Imaging Spectrograph (NIRIS). It is used to focus and orient each of NIRIS's three separate focal planes that together span the wavelength region from 0.38 μm to 2.5 μm. Procedures are also described for reducing and analyzing the measurement data.

The measurement concept for assessing focus and alignment is surprisingly simple given its diagnostic power. The entrance slit of a hyperspectral imager serves as its field stop. The portion of the field encompassed by the slit is re-imaged, in multiple dispersed colors, upon the FPA. A fore-optic, generally a telescope, forms the image of the field at the entrance slit. The fore-optic subtends a finite solid angle as viewed from the spectrograph. This solid angle is generally matched to the range of angles over which the spectrograph can accept light. This range of angles defines a cone, hereafter called the F-beam. In the absence of the foreoptic, small light sources in the far field will fill only a portion of the F-beam. This fact can be exploited to gauge focus because there is also an F-beam that is convergent upon the FPA with a direct correspondence to the F-beam in the far-field (In general, the opening angles of the two cones will not be equal because the collimator and camera focal lengths are generally not equal). If the system is properly focused, monochromatic light from all portions of the F-beam will converge at the same point on the focal plane. If not, the light from different portions will impinge on different locations on the FPA, but in a predictable way. For example, if the FPA is closer to the camera than the correct focus distance, light rays from opposite sides of the F-beam will fall at distinctly different locations. But because the two rays are on converging paths, they cross at focus, and their positions are switched beyond focus (see Figure 1). If the angle between the two rays is known and their location on the FPA can be measured, the change in the distance between the camera and the FPA necessary to bring the focal plane into correct focus can be calculated. This behavior is identical to that utilized by the classical knife-edge test—the additional power of the hyperspectral technique comes from employing multiple monochromatic sources (e.g., the atomic emission lines produced by a discharge lamp—Figures 2 and 3) over the long entrance slit to measure focus at many locations on the FPA simultaneously. The following sections describe how these measurements are made for the NIRIS spectrograph, how the data are reduced, and how they are analyzed.

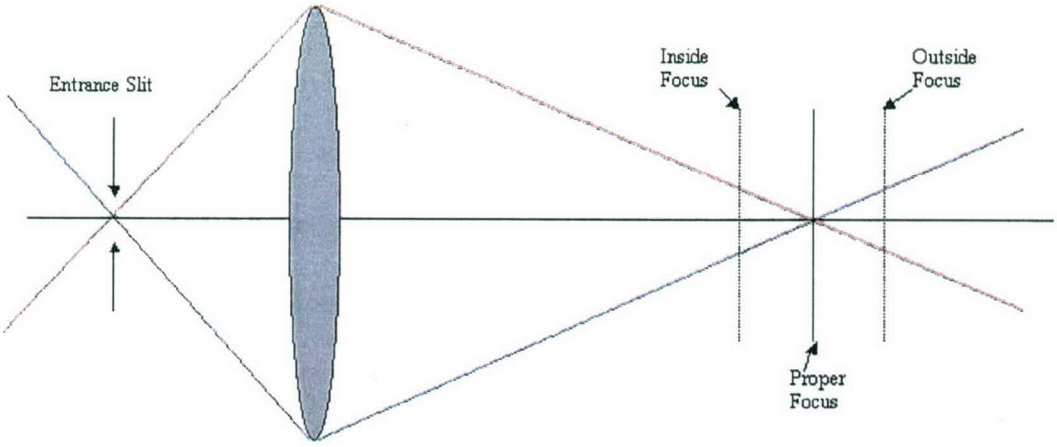

Figure 1. Simplified schematic illustrating the concept for testing focus. A light source is positioned at two locations in the sensor's F-beam (acceptance cone) in the far field (to the left of the entrance slit). Light from these positions follows the paths indicated by the red and blue rays. If the sensor is correctly focused, the plane denoted as "proper focus" is coincident with the detector array (FPA). If the FPA is located inside or outside of focus, the other cases result. Note, however, that regions where the red and blue paths intersect the FPA are reversed for the different cases. Note also that if the angle between the red and blue paths is known and their separation on the FPA is measured, the shift between the optics and the FPA necessary to obtain the best focus can be calculated.

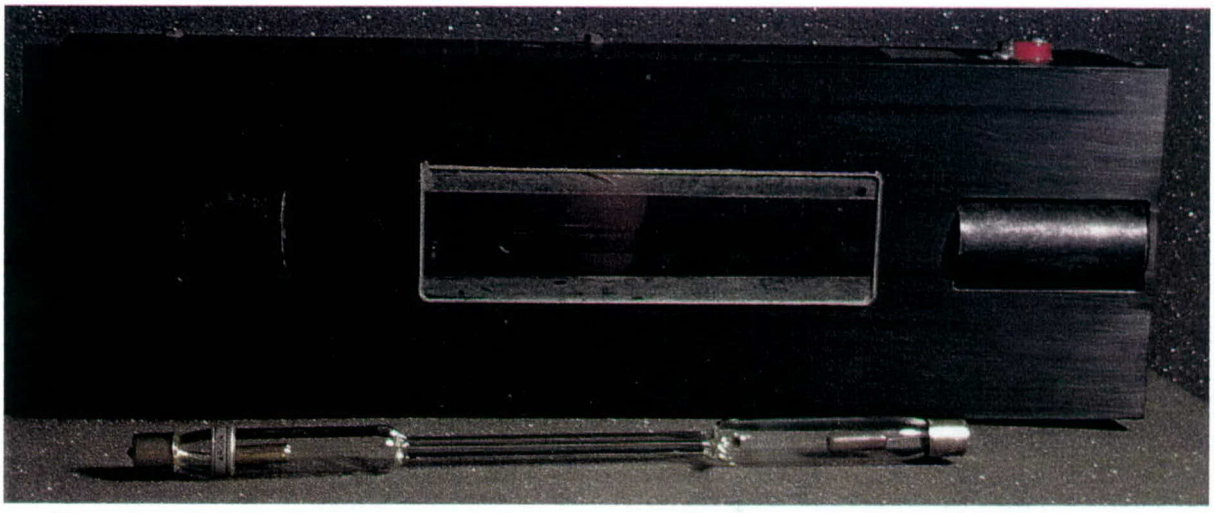

Figure 2. Emission lamp power supply, bulb, and cover. Supply uses standard 110 V AC. Discharge tubes include Hg, H, N, and O as well a variety of inert gases. Argon provides the largest number and best spread of strong emission lines for the red and near-IR.

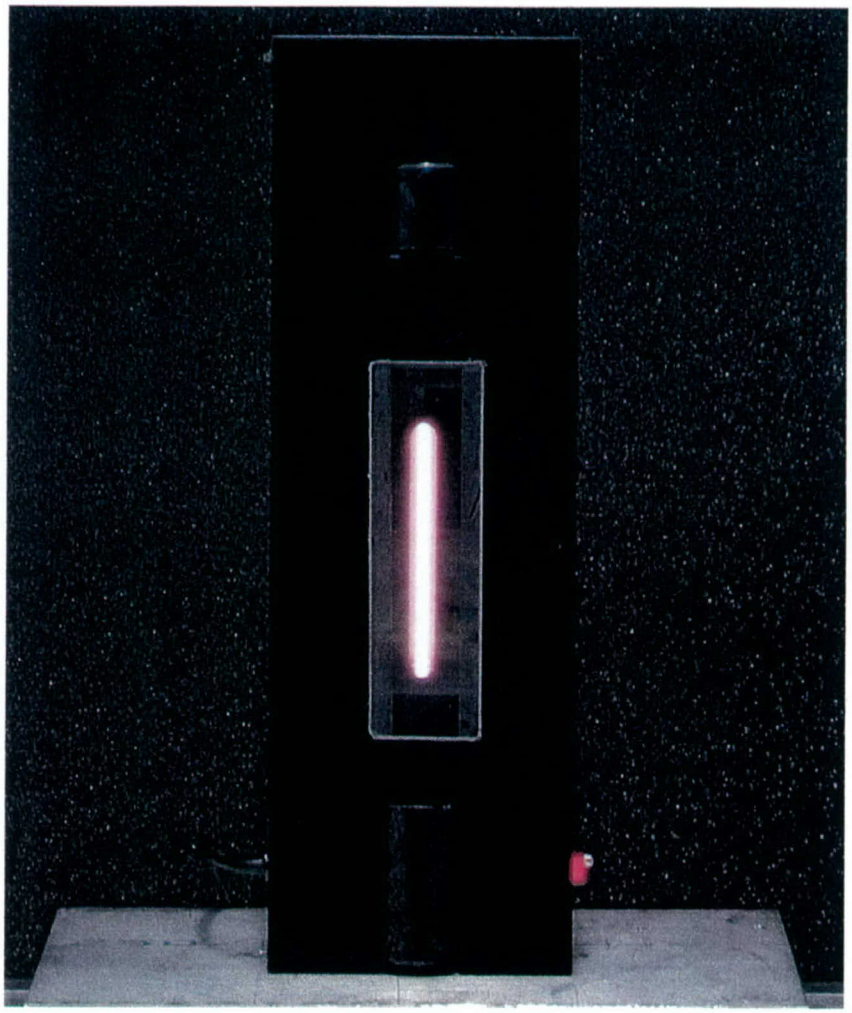

Figure 3. Discharge lamp operating with He bulb. The slightly pink color is due to the strong lines at 0.5876 and 0.7065 μm. Because the bulb case is quartz and the lamp has many strong features in the UV, it is covered by UV-blocking glass for eye protection.

2. Measurement Procedure

Below are the steps to obtain images of the wavelength calibration source at opposite sides of the F-beam.

1. Set-up the emission line lamp near the center of the spectrograph F-beam in the far field. The F-beam can be located well enough by finding the half-power points. Any source, including the emission lamp, can be used. This is a qualitative process; generally, visual observation of the output data is sufficient. This will also familiarize the experimenter with the appearance of the images.

2. Center the lamp near the mid-point in up/down direction and orient the long axis of the lamp parallel to the slit. (Here, we are assuming that the entrance slit of the spectrograph is vertical. If it is horizontal, the long axis of the lamp should be horizontal, and the lamp should be approximately centered right/left.)

3. Measure the distance between the spectrograph slit and the lamp.

4. Locate the half-power points in the left/right direction and mark them.

5. Mark points that are slightly inside the half-power points (approximately 1/10 of the separation between the half-power points). These will be the locations of the lamp for the measurements (see Figure 4). They are moved from the half-power points to ensure strong signals; the locations should be tweaked to produce spectra with well-defined lines and have comparable intensities.

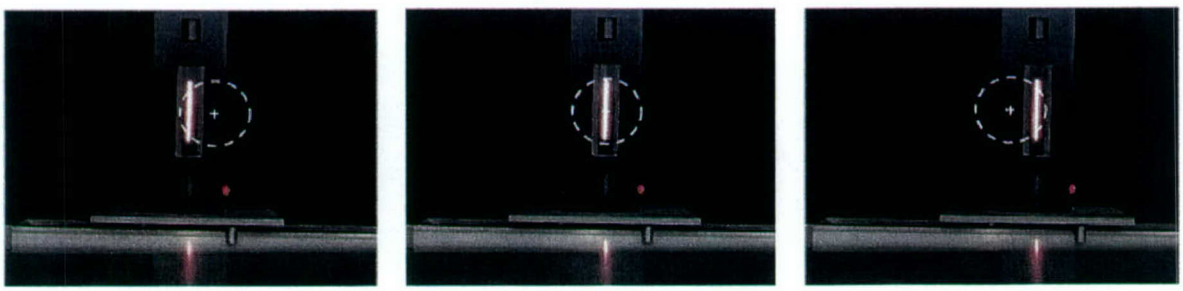

Figure 4. Right and left lamp positions for focus and orientation measurement (central position is shown for reference as well). The long axis of the lamp is parallel to the slit. The dashed circle represents the envelope of the spectrograph F-beam (the solid angle from over which the sensor can accept light). The lamps are positioned slightly inside the F-beam to ensure strong signals. The separation of the lamp in the left and right position divided by the distance of the lamp from the spectrograph entrance slit determines the crossing angle of the light paths on the focal plane. Use of the long lamp helps to uniformly illuminate the slit.

6. Measure the separation between the lamp locations.

7. Collect frames (i.e., hyperspectral images) with the lamp on and off at each of the two fiducial positions. The "off" frames provide for background subtraction, removing any stray emission lines that may arise from room lights or other fluorescent sources. The right and left images (minus their background images) are the data from which focus is measured and orthogonality is assessed.

3. Data Reduction Procedure

The goal of the data processing is to produce spectra from both the right and left lamp positions at selected positions along the slit. For this discussion, we will assume that the light is dispersed along the rows of the FPA and that columns parallel the slit. Here are the steps in the data reduction.

1. Subtract the background frames from their respective lamp images

2. Select a small number (5–20) of continuous rows from the center of the array. Collapse this array by coadding along columns to improve signal-to-noise ratio. This results in a spectrum for each of the lamp positions whose number of elements equals the dimension of the FPA in the spectral direction (Figure 5). Label these spectra "CR" and "CL" (for central rows and right and left).

3. Measure the positions (in pixel space) of the same emission lines for the spectra corresponding to the left and right lamp positions. Call these "CR_positions" and "CL_positions".

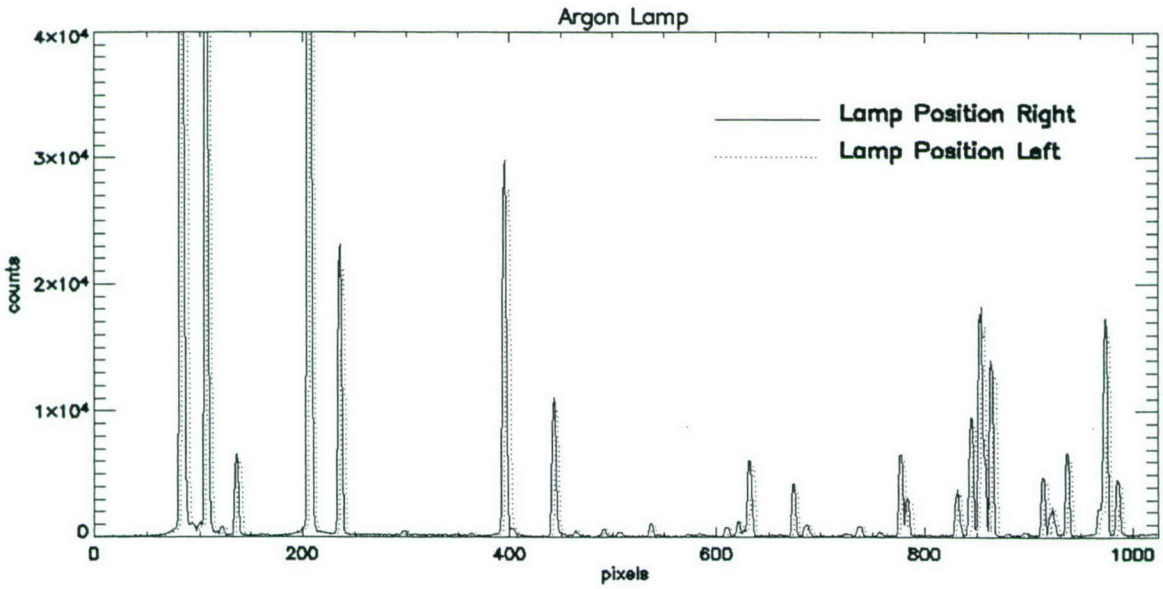

Figure 5. Argon spectrum in the 0.9–1.3 μm range. Spectra from both the lamp positions are plotted. The shift between them indicates a fairly substantial focus error. The emission lines are unresolved by the spectrograph, and their finite widths here represent the instrument resolution. A Gaussian fitting routine is used to determine the central position of each line.

4. Take the difference in the line positions between the left and right frames for all of the emission lines measured. Call this "C_differences," where C_differences = CR_positions – CL_positions.

5. Repeat steps 2–4 for a set of rows near the top and near the bottom of the array.

4. Data Analysis Procedure

This section assumes that there are 6 spectra (with background removed) resulting from the data reduction process—the left and right positions of the lamp at the center, top, and bottom of the array.

1. Determine the f-number of the experimental set-up. This is the separation between the right and left lamp positions divided by the distance between the slit and a line connecting the two lamp positions.

2. Determine the effective f-number of the experimental set-up *as seen by the focal plane.* This requires a knowledge of the optical design of the spectrograph. It should be very close to the experimental f-number times the ratio of the camera focal length to the collimator focal length. This is the "F-number" parameter for the calculation performed in step 4.

3. Find the average pixel shift of the emission lines between the right and left lamp positions for the spectra formed from the central rows of the array (as illustrated in Figures 6 and 7). This is the "Avg_Cdiff" parameter for the calculation performed in step 4.

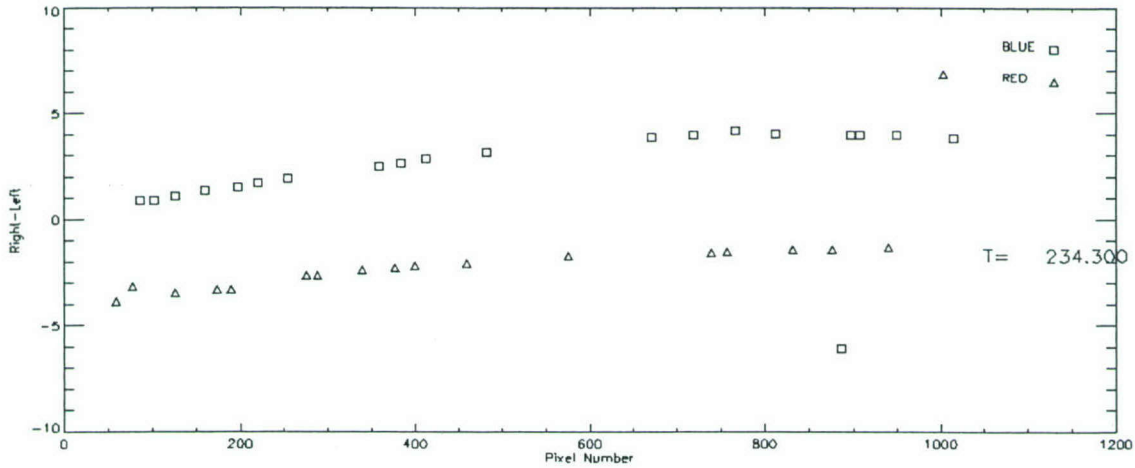

Figure 6. Results from a focus measurement for the two infrared channels of NIRIS. The "blue" channel covers the wavelength range 0.9–1.4 μm; the red spans 1.4–2.5 μm. Each square represents an emission line (of argon) measured by the blue channel; each triangle represents an argon line detected in red channel. The x-axis gives the location of the line in pixel number across the array (this corresponds to wavelength), which has 1024 pixels. The y-axis represents the difference in the location of line center with the lamp in the left and right positions. These data were acquired shortly after the spectrograph began cooling when the temperature of its optical bench (234.3K) was much warmer than its operational value (~145K). Both channels are far from focus (as gauged by the mean offset of the position differences from zero), and both show a slight slope. The latter indicates a small tilt (yaw deviation) of the FPA relative to the optical axis. The outlying points are due to misidentification of the emission line by the software.

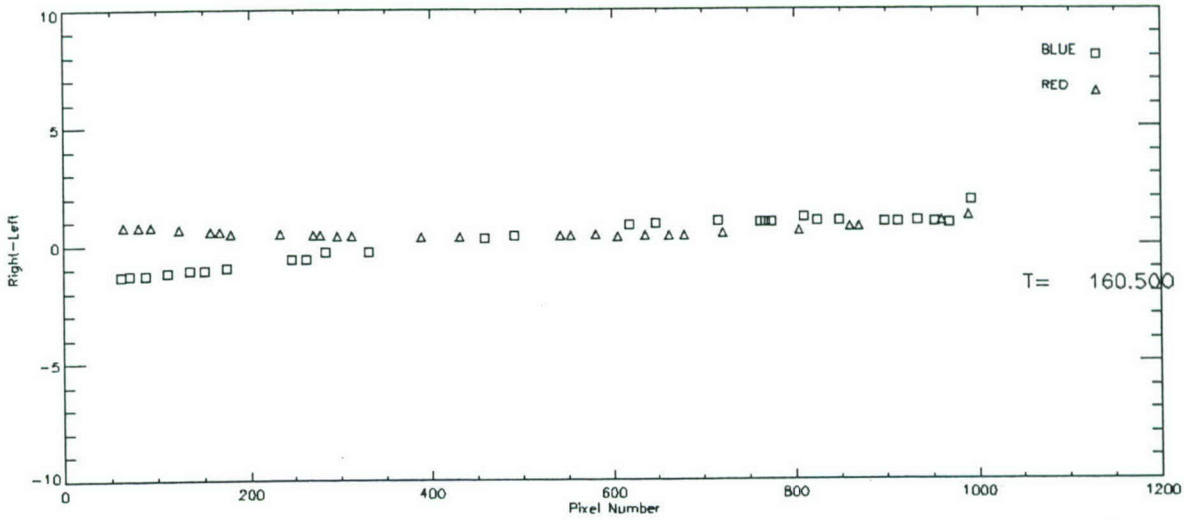

Figure 7. Same as Figure 4 but with an optical bench temperature (160.5K) much closer to nominal. The focus is nearly ideal for both channels, but the tilt is still present for the blue channel.

4. Compute the defocus distance, which is the amount that the separation between the spectrograph camera and the array should be changed to achieve the correct focus. This is equal to Avg_Cdiff x Pixel_size x F_number. Thus, a shift of 2 pixels in the position of the emission lines between the right and left lamp locations for an effective f-number of 3 for pixels 18.5 μm on a side (the value of the IR pixels in NIRIS) would indicate an error of 2 x 3 x 18.5 = 111 μm in the distance separating the camera and the FPA.

5. Determine the direction of defocus. This can be done by a careful ray trace that accounts for all the reflections and inversions in the optical train plus a precise understanding of the order in which the pixels of the FPA are read-out and concatenated. In practice, it is simpler to allow for one focus trial in which the shift has a 50% probability of being in the correct direction. If time is critical, as it may be for a cryogenic system where a warm-up must precede any focus adjustments, then spectra should be acquired both at the operating temperature and while cooling. The observed change in focus with temperature can then be compared with the predictions of the optical designer to determine the direction of the required focus motion.

6. Determine the error in tilt (yaw) of the FPA. A tilt in the FPA relative to the optical axis manifests as a systematic change in the shifts of the emission lines between the left and right lamp locations. For example, an FPA that is properly focused but has a tilt error could hit focus in the center while falling inside focus on one side and outside on the other. The angular error is just the slope in the pixel versus pixel difference plots (see Figure 6).

7. Determine the error in tip (pitch) of the FPA. A tip error in the FPA relative to the optical axis shows up as a change in the average shift of the emission lines from the top and bottom of the FPA. In this case, the center of the FPA is still in focus, but the top and bottom are out

of focus in different directions. The angular error is the focus difference between the top and bottom sections of the array divided by their mean separation (in pixels).

8. Estimate the roll of the FPA about the optical axis. This is done by observing the orientation of emission lines in either of the right or left hyperspectral images. Because the slit is fully illuminated, the emission lines will extend from the top to the bottom of the array and may be checked for general alignment with FPA columns. In the ideal case, the emission lines would be vertical, tracking the columns, while the dispersion would be horizontal, aligned with the rows. However, the orientation of the emission lines on the array is determined by the orientation of the slit, whereas the dispersion direction is dictated by the grating or dispersive element. Non-planar reflections by the optics that re-image the slit on the FPA can rotate its projection such that the spatial and spectral dimensions are no longer perpendicular. Determining the angle between the dispersive direction and the rows of the array is best done by imaging a point source on the slit.

5. Summary

This document has described a process for focusing and aligning a hyperspectral imager. While the examples and results presented here are for a specific instrument operating in the 0.38-2.5 micron wavelength region, the technique is applicable to any long-slit spectrograph where the F-beam is accessible and a suitable wavelength calibration source exists. The only special equipment required is the spectrograph under test, its data acquisition system, and the calibration source. Specific procedures have been given for acquiring, reducing, and analyzing the data.

LABORATORY OPERATIONS

The Aerospace Corporation functions as an "architect-engineer" for national security programs, specializing in advanced military space systems. The Corporation's Laboratory Operations supports the effective and timely development and operation of national security systems through scientific research and the application of advanced technology. Vital to the success of the Corporation is the technical staff's wide-ranging expertise and its ability to stay abreast of new technological developments and program support issues associated with rapidly evolving space systems. Contributing capabilities are provided by these individual organizations:

Electronics and Photonics Laboratory: Microelectronics, VLSI reliability, failure analysis, solid-state device physics, compound semiconductors, radiation effects, infrared and CCD detector devices, data storage and display technologies; lasers and electro-optics, solid-state laser design, micro-optics, optical communications, and fiber-optic sensors; atomic frequency standards, applied laser spectroscopy, laser chemistry, atmospheric propagation and beam control, LIDAR/LADAR remote sensing; solar cell and array testing and evaluation, battery electrochemistry, battery testing and evaluation.

Space Materials Laboratory: Evaluation and characterizations of new materials and processing techniques: metals, alloys, ceramics, polymers, thin films, and composites; development of advanced deposition processes; nondestructive evaluation, component failure analysis and reliability; structural mechanics, fracture mechanics, and stress corrosion; analysis and evaluation of materials at cryogenic and elevated temperatures; launch vehicle fluid mechanics, heat transfer and flight dynamics; aerothermodynamics; chemical and electric propulsion; environmental chemistry; combustion processes; space environment effects on materials, hardening and vulnerability assessment; contamination, thermal and structural control; lubrication and surface phenomena. Microelectromechanical systems (MEMS) for space applications; laser micromachining; laser-surface physical and chemical interactions; micropropulsion; micro- and nanosatellite mission analysis; intelligent microinstruments for monitoring space and launch system environments.

Space Science Applications Laboratory: Magnetospheric, auroral and cosmic-ray physics, wave-particle interactions, magnetospheric plasma waves; atmospheric and ionospheric physics, density and composition of the upper atmosphere, remote sensing using atmospheric radiation; solar physics, infrared astronomy, infrared signature analysis; infrared surveillance, imaging and remote sensing; multispectral and hyperspectral sensor development; data analysis and algorithm development; applications of multispectral and hyperspectral imagery to defense, civil space, commercial, and environmental missions; effects of solar activity, magnetic storms and nuclear explosions on the Earth's atmosphere, ionosphere and magnetosphere; effects of electromagnetic and particulate radiations on space systems; space instrumentation, design, fabrication and test; environmental chemistry, trace detection; atmospheric chemical reactions, atmospheric optics, light scattering, state-specific chemical reactions, and radiative signatures of missile plumes.